

A new approach for graph signal separation based on smoothness

Mohammad-Hassan Ahmad Yarandi, Massoud Babaie-Zadeh

Abstract—Blind source separation (BSS) is a signal processing subject that has recently been extended to graph signals. Graph signals that are smooth on their own graphs provide an opportunity to separate them from their summation by knowing their underlying graphs, which is different from the conventional BSS that requires at least two mixtures of source signals. In this paper, we introduce an approach to separate smooth graph signals whose energy is concentrated on their first frequency components. This approach tries to decompose the summation signal into signals that are as smooth as possible on their underlying graphs and non-smooth on the other graphs. Moreover, in the case that the number of source signals is two, the uniqueness of our separation approach is shown, up to the uncertainty of the average value of the signals. Furthermore, we interpret the solution of our approach in the case of complement graphs by deriving exact error formulas. Finally, simulations demonstrate the efficiency of the proposed approach and its superiority over other approaches in this setting.

Index Terms—graph signal processing, graph signal separation, blind source separation, smooth graph signal.

I. INTRODUCTION

GRAPH Signal Processing (GSP) [1] is an emerging field that investigates signals arising from complex structures, modeled by graphs. Compared with classic signal processing, this graph structure can consider connections between every pair of signal samples, which can improve the processing of signals. In some applications, *e.g.* social networks and transportation networks, the graph is known a priori, while in other applications the graph is to be learned from a database of signals according to the relations and similarities between their samples [2].

Many topics in classic signal processing have been extended to graph signal processing. A topic that has recently been generalized to GSP is Blind Source Separation (BSS) [3]. The main goal of BSS is to recover statistically independent source signals from their mixtures, and has a wide range of applications from biomedical signals to stock prediction [3]. In classical BSS, the number of mixed signals is typically assumed to be greater than or equal to the number of source signals.

In [4]–[7], two BSS methods for graph signals, GraphJADE and Graph Decorrelation, are proposed based on graph decorrelation information along with conventional BSS objective functions. Both methods require the underlying graphs as prior information. In the case that the graphs are unknown, the authors of [8] and [9] propose methods that learn the underlying graphs and separate the graph signals simultaneously. In another approach in [10], the smoothness criteria

of graph signals are used as regularization terms along with a mutual information based cost function to separate smooth graph signals. Similarly in [11], this method is extended to a method that jointly learns the graphs and separates the graph signals. In all the above mentioned methods, similar to most classical BSS methods, the number of available mixed signals is assumed to be equal to the number of source signals.

There are however papers that address the graph signal separation problem in a different setting. In this setting, there is *only one mixture* of source signals that is equal to their summation. These approaches impose other assumptions on source signals, *e.g.* their smoothness or their generation process. These assumptions distinguish each signal on their underlying graph from other signals and enable the separation from only one mixture. In [12], [13], the assumption is that each graph signal is generated from a diffusion process with a sparse input via a graph filter with unknown coefficients. In [14], the assumption is that each graph signal is smooth on its graph or has sparse frequency components. More precisely, consider K unknown graph signals $\mathbf{x}_1, \dots, \mathbf{x}_K$ with corresponding known graphs $\mathcal{G}_1, \dots, \mathcal{G}_K$. The known graphs $\mathcal{G}_1, \dots, \mathcal{G}_K$ have the same node set and are different only in their edge sets and adjacency matrices. Each graph signal is assumed to be smooth and approximately bandlimited on its graph.¹ The only observed signal is the summation signal $\mathbf{x} \triangleq \sum_{i=1}^K \mathbf{x}_i$ and the goal is to recover $\mathbf{x}_1, \dots, \mathbf{x}_K$ from \mathbf{x} . Then, [14] proposes separation methods by exploiting the smoothness (or the sparsity) of each graph signal on its corresponding graph. The closed-form solutions and estimation errors of the methods in [14] are given in [17].

In this paper, a new separation approach is proposed to enhance the quality of the separation methods of [14]. Our approach is based on considering the smoothness of each graph signal \mathbf{x}_i on both its corresponding graph \mathcal{G}_i and the graphs of the other signals \mathcal{G}_j , $j \neq i$. Indeed, it is based on the assumption that each graph signal is smooth on its corresponding graph and non-smooth on the other graphs. Therefore, this approach tries to recover the graph signals from their summation \mathbf{x} such that the obtained signals are as smooth as possible on their own graphs and non-smooth on the other graphs. The main contributions of this article are as follows:

- Based on additional consideration of the smoothness criteria of graph signals on the graph of other signals alongside their corresponding graphs, new methods are proposed for both noiseless and noisy data, which outperform previous methods.

Department of Electrical Engineering, Sharif University of Technology, Tehran, Iran (e-mail: mh.ahmad.yarandi@gmail.com, mbzadeh@yahoo.com).

¹Smooth and bandlimited graph signals appear in some applications like graphs with k clusters, where the signals within each cluster are smooth [15], [16].

- In case of $K = 2$, the uniqueness of our separation method with noiseless data is shown up to the indeterminacy of the average values of the signals. Additionally, a fixed point algorithm is proposed in this case.
- In case of complement graphs, closed-form formulas are derived for the estimation error of both our method and the method of [14].

In simulations, the performance of our methods is evaluated, and they are compared with the methods of [14], which up to our best knowledge is the only paper in the same problem formulation as this paper.

The rest of the paper is organized as follows. In Section II, a brief background on GSP is reviewed. In Section III, our proposed approach is introduced in different cases along with a uniqueness theorem. Estimation error formulas are provided for the case of complement graphs in Section IV. Finally, Section V is devoted to numerical experiments.

II. GSP BACKGROUND

An undirected graph with N nodes can be represented as $\mathcal{G} = (\mathcal{V}, \mathcal{E}, \mathbf{W})$, where \mathcal{V} is the set of nodes ($|\mathcal{V}| = N$), $\mathcal{E} \subseteq \mathcal{V} \times \mathcal{V}$ is the set of edges, and $\mathbf{W} \in \mathbb{R}^{N \times N}$ is the weight matrix. For undirected graphs with no self-loop, \mathbf{W} is a symmetric matrix whose diagonal entries are equal to zero. For binary graphs, the entries of \mathbf{W} indicate the presence or absence of the edge between each pair of the nodes and in weighted graphs, they also determine the weight of each edge. A graph signal $\mathbf{x} \in \mathbb{R}^N$ is a mapping from the node set to \mathbb{R}^N that assigns a real value x_i to the node i for $i = 1, \dots, N$. In this paper, the problem consists of K known graphs $\mathcal{G}_i = (\mathcal{V}, \mathcal{E}_i, \mathbf{W}_i)$ for $i = 1, \dots, K$ that have the same node set, and their difference is only in their edge set and weight matrix. On each graph, there is a graph signal \mathbf{x}_i that has a specific structure and the goal is to reconstruct these signals from their summation $\mathbf{x} \triangleq \sum_{i=1}^K \mathbf{x}_i$.

Another matrix by which a graph can be described is the Laplacian matrix, defined as $\mathbf{L} \triangleq \mathbf{D} - \mathbf{W}$, where \mathbf{W} is the weight matrix and \mathbf{D} is the degree matrix defined as $\mathbf{D} \triangleq \text{diag}(\mathbf{W}\mathbf{1})$, in which $\mathbf{1} \triangleq [1, \dots, 1]^T \in \mathbb{R}^N$ stands for the all-one vector. Smoothness of a graph signal shows the variation of the signal values on the graph and can be measured by the graph Laplacian quadratic form as

$$\mathbf{x}^T \mathbf{L} \mathbf{x} = \sum_{1 \leq i < j \leq N} w_{ij} (x_i - x_j)^2. \quad (1)$$

From the above equation, it is obvious that \mathbf{L} is a positive semidefinite matrix, and its smallest eigenvalue is equal to zero with the corresponding eigenvector $\mathbf{1}$ (for connected graphs, only one of the eigenvalues is equal to zero [1]). Hence, it has eigenvalues $0 = \lambda_1 \leq \dots \leq \lambda_N$ and N orthonormal eigenvectors $\mathbf{v}_1, \dots, \mathbf{v}_N$ and therefore, the eigenvalue decomposition of \mathbf{L} is in the form $\mathbf{L} = \mathbf{V} \mathbf{\Lambda} \mathbf{V}^T$, where $\mathbf{\Lambda} \triangleq \text{diag}(\lambda_1, \dots, \lambda_N)$ and $\mathbf{V} \triangleq [\mathbf{v}_1, \dots, \mathbf{v}_N]$. For a graph signal $\mathbf{x} \in \mathbb{R}^N$, the Graph Fourier Transform (GFT) is defined as $\hat{\mathbf{x}} \triangleq \mathbf{V}^T \mathbf{x}$, with respect to \mathbf{L} as shift operator. Similarly, the Inverse Graph Fourier Transform (IGFT) is defined as $\mathbf{x} \triangleq \mathbf{V} \hat{\mathbf{x}}$. With these definitions, noting that $\mathbf{v}_i^T \mathbf{L} \mathbf{v}_i = \lambda_i$, the λ_i 's represent

frequencies in the GFT domain, *i.e.* the smaller λ_i 's shows that the corresponding eigenvectors are smoother on the graph. The following equation shows smoothness in the frequency domain:

$$\mathbf{x}^T \mathbf{L} \mathbf{x} = \sum_{1 \leq i \leq N} \lambda_i \hat{x}_i^2, \quad (2)$$

where \hat{x}_i is the i -th frequency component of \mathbf{x} , corresponding to the frequency λ_i . Since for smooth graph signals $\mathbf{x}^T \mathbf{L} \mathbf{x} = \epsilon$ is small, $|\hat{x}_i| < \frac{\epsilon}{\lambda_i}$. Therefore, in the GFT domain, the GFT coefficients of a smooth graph signal should be small in high frequencies and can be large in lower frequencies. In this paper, we consider smooth signals as signals with GFT coefficients concentrated on the low frequencies, such as the combination of a few first eigenvectors of the Laplacian matrix.

According to the eigenvalue decomposition, the Laplacian matrix can be written in the form $\mathbf{L} = \sum_{i=1}^N \lambda_i \mathbf{v}_i \mathbf{v}_i^T$, and its Moore–Penrose pseudo inverse can be defined as $\mathbf{L}^\dagger = \sum_{i=2}^N \frac{1}{\lambda_i} \mathbf{v}_i \mathbf{v}_i^T$. Since the Laplacian matrix of connected graphs has exactly one zero eigenvalue, which corresponds to the direction of the all-one vector, the system of linear equations $\mathbf{L} \mathbf{x} = \mathbf{y}$ has several solutions that differ only in the average value of \mathbf{x} , and $\mathbf{L}^\dagger \mathbf{x}$ is the solution whose average is equal to zero. In this paper, the average value of a graph signal \mathbf{x} is referred as its DC value, that is, $\bar{x} \triangleq \frac{1}{N} \sum_{i=1}^N x_i = \frac{1}{\sqrt{N}} \hat{x}_1$.

III. THE PROPOSED METHOD

In this section, the problem of graph signal separation in the case of two graphs is considered. So, there are two unknown graph signals \mathbf{x}_1 and \mathbf{x}_2 that are smooth on their known graphs (having the same nodes), and the goal is to recover these signals from their known summation $\mathbf{x} \triangleq \mathbf{x}_1 + \mathbf{x}_2$. At first, the methods of [14] are very briefly reviewed, and then our proposed method in both noiseless and noisy settings are stated. Finally, our method is generalized to the case of more than two graphs.

A. A brief review on the methods of [14]

Consider two graphs \mathcal{G}_1 and \mathcal{G}_2 with the same nodes and with corresponding Laplacian matrices \mathbf{L}_1 and \mathbf{L}_2 . Suppose that \mathbf{x}_1 and \mathbf{x}_2 are smooth signals on \mathcal{G}_1 and \mathcal{G}_2 . For recovering these signals from $\mathbf{x} = \mathbf{x}_1 + \mathbf{x}_2$, the authors of [14] propose the optimization problem

$$\underset{\mathbf{x}_1, \mathbf{x}_2}{\text{minimize}} \quad \mathbf{x}_1^T \mathbf{L}_1 \mathbf{x}_1 + \mathbf{x}_2^T \mathbf{L}_2 \mathbf{x}_2 \quad \text{s.t.} \quad \mathbf{x} = \mathbf{x}_1 + \mathbf{x}_2. \quad (3)$$

As stated in [14, Theorem 1], the solution of (3) is unique up to the DC values of \mathbf{x}_1 and \mathbf{x}_2 . Therefore, a unique solution can be obtained without considering the DC values of the signals. Thus, [14] proposes the following problem whose solution is unique:

$$\underset{\mathbf{x}_1, \mathbf{x}_2}{\text{minimize}} \quad \mathbf{x}_1^T \mathbf{L}_1 \mathbf{x}_1 + \mathbf{x}_2^T \mathbf{L}_2 \mathbf{x}_2 \quad \text{s.t.} \quad \begin{cases} \mathbf{z} = \mathbf{x}_1 + \mathbf{x}_2, \\ \bar{x}_1 = \bar{x}_2 = 0, \end{cases} \quad (4)$$

where $\mathbf{z} \triangleq \mathbf{x} - \bar{x} \mathbf{1}$.

As shown in [14], based on (2), problem (4) can be written in the GFT domain as

$$\underset{\hat{\mathbf{x}}_1, \hat{\mathbf{x}}_2}{\text{minimize}} \quad \sum_{i=2}^N \lambda_{1i} \hat{x}_{1i}^2 + \lambda_{2i} \hat{x}_{2i}^2 \quad \text{s.t.} \quad \begin{cases} \mathbf{z} = \mathbf{V}_1 \hat{\mathbf{x}}_1 + \mathbf{V}_2 \hat{\mathbf{x}}_2, \\ \hat{x}_{11} = \hat{x}_{21} = 0, \end{cases} \quad (5)$$

where $\mathbf{L}_j = \mathbf{V}_j \mathbf{\Lambda}_j \mathbf{V}_j^T$ is the eigenvalue decomposition of \mathbf{L}_j , $j = 1, 2$, $\hat{\mathbf{x}}_j = \mathbf{V}_j^T \mathbf{x}_j = [\hat{x}_{j1}, \dots, \hat{x}_{jN}]$ is the GFT of \mathbf{x}_j based on \mathbf{L}_j , and λ_{ji} is the i -th eigenvalue of \mathbf{L}_j .

As discussed in [14], for two graphs with very different eigenvalue distributions, problem (5) does not give the same importance to the corresponding frequency components of two signals and hence the solution of (5) may not be accurate enough. So, [14] proposes to use the positive weights $w_2 < \dots < w_N$ instead of the eigenvalues of two graphs to give the same importance to the frequency components in both graphs. One suggestion for the weights in [14] is $w_i = (i-2) \times s + 1$ for some $s > 0$. Hence, problem (5) is reformulated in [14] as

$$\underset{\hat{\mathbf{x}}_1, \hat{\mathbf{x}}_2}{\text{minimize}} \quad \sum_{i=2}^N w_i (\hat{x}_{1i}^2 + \hat{x}_{2i}^2) \quad \text{s.t.} \quad \begin{cases} \mathbf{z} = \mathbf{V}_1 \hat{\mathbf{x}}_1 + \mathbf{V}_2 \hat{\mathbf{x}}_2, \\ \hat{x}_{11} = \hat{x}_{21} = 0. \end{cases} \quad (6)$$

According to the description in [14], problem (6) can also be used in the case of separating signals that are not necessarily smooth but have the same known frequency support. In this case, the weights w_2, \dots, w_N are chosen in a way that for the support frequencies, the weights are small and for other frequencies are large.

B. Our proposed approach

A common property in all the problems of [14] is that the objective functions only focus on the smoothness of each signal on its own graph. Therefore, the solutions of these methods may be signals that are smooth not only on the corresponding graphs but also on the graphs of the others. However, if the graphs are different enough, it is reasonable to assume that the source signals (assumed to be smooth on their own graphs) are non-smooth on the graphs of the other signals. This is because these smooth signals are concentrated in the lower frequencies of their own graphs, which is likely to not correspond to the lower frequencies of the other graphs (due to the differences between the graphs. An extreme case will be seen in Section IV). Therefore, to separate these signals, the objective function would be better to take into account the non-smoothness of each signal on the graphs of the other signals along with its smoothness on its own graph. In this paper, the proposed optimization problem is

$$\underset{\mathbf{x}_1, \mathbf{x}_2}{\text{minimize}} \quad \frac{\mathbf{x}_1^T \mathbf{L}_1 \mathbf{x}_1 + \mathbf{x}_2^T \mathbf{L}_2 \mathbf{x}_2}{\mathbf{x}_1^T \tilde{\mathbf{L}}_2 \mathbf{x}_1 + \mathbf{x}_2^T \tilde{\mathbf{L}}_1 \mathbf{x}_2} \quad \text{s.t.} \quad \mathbf{x} = \mathbf{x}_1 + \mathbf{x}_2. \quad (7)$$

The purpose of this objective function is to find graph signals \mathbf{x}_1 and \mathbf{x}_2 that are as smooth as possible on their own graphs and non-smooth on the graph of the other one. This approach is similar to Linear Discriminant Analysis (LDA) [18], which is used to project data from multiple groups from a higher dimensional space into a lower dimensional space such that

the data of one group are as close as possible to each other and are far from the data of the other groups.

Similar to problem (3), it can be shown that problem (7) has a unique solution up to the DC values of the signals under a mild condition:

Theorem 1. *If \mathcal{G}_1 and \mathcal{G}_2 are two connected graphs with the same nodes, and if $\mathbf{L}_1 \mathbf{x} \neq \mathbf{L}_2 \mathbf{x}$, then the solutions of problem (7) differ only in their DC values (i.e. they are unique up to the DC values of \mathbf{x}_1 and \mathbf{x}_2).*

The proof is left to Appendix A.

Therefore, when $\mathbf{L}_1 \mathbf{x} \neq \mathbf{L}_2 \mathbf{x}$, by constraining the DC values of the signals equal to zero and defining $\mathbf{z} = \mathbf{x} - \bar{x} \mathbf{1}$, the solution of the following problem is unique:

$$\underset{\mathbf{x}_1, \mathbf{x}_2}{\text{minimize}} \quad \frac{\mathbf{x}_1^T \mathbf{L}_1 \mathbf{x}_1 + \mathbf{x}_2^T \mathbf{L}_2 \mathbf{x}_2}{\mathbf{x}_1^T \mathbf{L}_2 \mathbf{x}_1 + \mathbf{x}_2^T \mathbf{L}_1 \mathbf{x}_2} \quad \text{s.t.} \quad \begin{cases} \mathbf{z} = \mathbf{x}_1 + \mathbf{x}_2, \\ \bar{x}_1 = \bar{x}_2 = 0. \end{cases} \quad (8)$$

Similar to problem (5), problem (8) can be written in the GFT domain and the modification used in problem (6) can be used here as well. To do so, instead of $\mathbf{L}_i = \mathbf{V}_i \mathbf{\Lambda}_i \mathbf{V}_i^T$, we use $\tilde{\mathbf{L}}_i = \mathbf{V}_i \text{diag}(0, w_2, \dots, w_N) \mathbf{V}_i^T$, which is not necessarily a valid graph Laplacian matrix. However, it refines the drawback of problem (8), which as stated for problem (5), happens in the case of two graphs with very different eigenvalue distributions. This technique also improves the separation performance in cases that $\lambda_{\max}(\mathbf{L}_i)/\lambda_2(\mathbf{L}_i)$ is low. Therefore, problem (8) can be represented as

$$\underset{\mathbf{x}_1, \mathbf{x}_2}{\text{minimize}} \quad \frac{\mathbf{x}_1^T \tilde{\mathbf{L}}_1 \mathbf{x}_1 + \mathbf{x}_2^T \tilde{\mathbf{L}}_2 \mathbf{x}_2}{\mathbf{x}_1^T \tilde{\mathbf{L}}_2 \mathbf{x}_1 + \mathbf{x}_2^T \tilde{\mathbf{L}}_1 \mathbf{x}_2} \quad \text{s.t.} \quad \begin{cases} \mathbf{z} = \mathbf{x}_1 + \mathbf{x}_2, \\ \bar{x}_1 = \bar{x}_2 = 0. \end{cases} \quad (9)$$

Remark 1: Similar to problem (6), problem (9) can also be used in the case of separating signals with the same limited known frequency supports that are not necessarily smooth. In this case, the eigenvectors corresponding to the support frequencies play the role of low-frequency eigenvectors, and the problem becomes similar to the separation of smooth graph signals.

Remark 2: The assumption $\mathbf{L}_1 \mathbf{x} \neq \mathbf{L}_2 \mathbf{x}$ is necessary for Theorem 1 since if $\mathbf{L}_1 \mathbf{x} = \mathbf{L}_2 \mathbf{x}$, then by simple calculations, it can be seen that

$$(\mathbf{x}_1^*)^T \mathbf{L}_1 \mathbf{x}_1^* + (\mathbf{x}_2^*)^T \mathbf{L}_2 \mathbf{x}_2^* = (\mathbf{x}_1^*)^T \mathbf{L}_2 \mathbf{x}_1^* + (\mathbf{x}_2^*)^T \mathbf{L}_1 \mathbf{x}_2^*,$$

where $(\mathbf{x}_1^*, \mathbf{x}_2^*)$ are the source signals. Therefore, in this case, the solution of the problem (8) is not unique.

Remark 3: Since in the proof of Theorem 1, only the semi-positive definiteness property of the matrices and the uniqueness of zero eigenvalue (which is equivalent to the connectivity of the graphs) are used, the solution of problem (9) is also unique when $\tilde{\mathbf{L}}_1 \mathbf{x} \neq \tilde{\mathbf{L}}_2 \mathbf{x}$.

C. A fixed point algorithm

By using Karush-Kuhn-Tucker (KKT) conditions [19] in problem (7), a fixed point algorithm that has a fast convergence

Algorithm 1 Fixed Point Algorithm for Problem (8)

 INPUT: $\mathbf{x}_1, \mathbf{z} \in \mathbb{R}^N, \mathbf{L}_1, \mathbf{L}_2$

 OUTPUT: $\mathbf{x}_1^*, \mathbf{x}_2^* \in \mathbb{R}^N$
repeat

$$\mathbf{x}_1 \leftarrow (\mathbf{L}_1 + \mathbf{L}_2)^\dagger \frac{(\mathbf{L}_2 - J(\mathbf{x}_1, \mathbf{z} - \mathbf{x}_1)\mathbf{L}_1)\mathbf{z}}{1 - J(\mathbf{x}_1, \mathbf{z} - \mathbf{x}_1)}$$

until convergence
If $J(\mathbf{x}_1, \mathbf{z} - \mathbf{x}_1) < 1$ **return** $\mathbf{x}_1^* = \mathbf{x}_1, \mathbf{x}_2^* = \mathbf{z} - \mathbf{x}_1$
If $J(\mathbf{x}_1, \mathbf{z} - \mathbf{x}_1) > 1$ **return** $\mathbf{x}_1^* = \mathbf{z} - \mathbf{x}_1, \mathbf{x}_2^* = \mathbf{x}_1$

rate can be obtained to solve problems (8) and similarly (9). The KKT conditions of (7) are written as

$$\begin{cases} 2 \frac{\mathbf{L}_1 \mathbf{x}_1 - J(\mathbf{x}_1, \mathbf{x}_2) \mathbf{L}_2 \mathbf{x}_1}{\mathbf{x}_1^T \mathbf{L}_2 \mathbf{x}_1 + \mathbf{x}_2^T \mathbf{L}_1 \mathbf{x}_2} + \boldsymbol{\mu} = \mathbf{0} \\ 2 \frac{\mathbf{L}_2 \mathbf{x}_2 - J(\mathbf{x}_1, \mathbf{x}_2) \mathbf{L}_1 \mathbf{x}_2}{\mathbf{x}_1^T \mathbf{L}_2 \mathbf{x}_1 + \mathbf{x}_2^T \mathbf{L}_1 \mathbf{x}_2} + \boldsymbol{\mu} = \mathbf{0} \\ \mathbf{x}_1 + \mathbf{x}_2 = \mathbf{x} \end{cases}, \quad (10)$$

where $\boldsymbol{\mu} \in \mathbb{R}^N$ is the vector of Lagrange multipliers and $J(\mathbf{x}_1, \mathbf{x}_2)$ denotes the objective function of (7). Combining the first two conditions in (10) results in

$$\mathbf{L}_1 \mathbf{x}_1 - J(\mathbf{x}_1, \mathbf{x}_2) \mathbf{L}_2 \mathbf{x}_1 = \mathbf{L}_2 \mathbf{x}_2 - J(\mathbf{x}_1, \mathbf{x}_2) \mathbf{L}_1 \mathbf{x}_2. \quad (11)$$

Now, using the third condition in the above equation leads to

$$\mathbf{x}_1 = (\mathbf{L}_1 + \mathbf{L}_2)^\dagger \frac{(\mathbf{L}_2 - J(\mathbf{x}_1, \mathbf{x} - \mathbf{x}_1)\mathbf{L}_1)\mathbf{x}}{1 - J(\mathbf{x}_1, \mathbf{x} - \mathbf{x}_1)} \triangleq f(\mathbf{x}_1). \quad (12)$$

Therefore, the fixed-point iterative algorithm

$$\mathbf{x}_1^{(i)} = f(\mathbf{x}_1^{(i-1)}), \quad i = 1, 2, \dots,$$

can be used to find \mathbf{x}_1 . Due to the term $(\mathbf{L}_1 + \mathbf{L}_2)^\dagger$ in f for every starting point $\mathbf{x}_1^{(0)}$, the DC value of $\mathbf{x}_1^{(i)}$ is equal to zero in each iteration. In order to use this algorithm to solve problem (8), it is enough to change \mathbf{x} to \mathbf{z} in f . Therefore, in each iteration, $\mathbf{x}_1^{(i)}$ and $\mathbf{x}_2^{(i)} = \mathbf{z} - \mathbf{x}_1^{(i)}$ are zero mean vectors and $\mathbf{x}_1^{(i)} + \mathbf{x}_2^{(i)} = \mathbf{z}$. Since $\mathbf{x}_1^{(i)}$ may converge to the maximum point, at the end, when $\mathbf{x}_1^{(i)}$ converges to \mathbf{x}_1 , it should be checked that $J(\mathbf{x}_1, \mathbf{z} - \mathbf{x}_1)$ is greater than one or not. If $J(\mathbf{x}_1, \mathbf{z} - \mathbf{x}_1) > 1$, then $(\mathbf{x}_1, \mathbf{z} - \mathbf{x}_1)$ is declared as the maximum point and $(\mathbf{z} - \mathbf{x}_1, \mathbf{x}_1)$ as the minimum point. Putting these together results in an algorithm for solving (8), which is summarized in Algorithm 1. Based on simulations, this algorithm converges to the optimal point. For a faster convergence rate it is better to consider the solution of problem (4) as an initial point for \mathbf{x}_1 , which is presented as a closed-form solution in [17]. Moreover, to solve problem (9) by Algorithm 1, it is enough to consider $\tilde{\mathbf{L}}_1, \tilde{\mathbf{L}}_2$ instead of $\mathbf{L}_1, \mathbf{L}_2$ as inputs.

D. Generalization to the case of noisy data and more than two sources

In the case of the presence of noise in \mathbf{x} , problem (7) can be modified such that its constraints are added to the objective function as a regularization term. Suppose that $\mathbf{x} = \mathbf{x}_1 + \mathbf{x}_2 +$

\mathbf{n} , where \mathbf{n} is a noise vector. So, we propose to replace (7) by

$$\underset{\mathbf{x}_1, \mathbf{x}_2}{\text{minimize}} \quad \frac{\mathbf{x}_1^T \mathbf{L}_1 \mathbf{x}_1 + \mathbf{x}_2^T \mathbf{L}_2 \mathbf{x}_2}{\mathbf{x}_1^T \mathbf{L}_2 \mathbf{x}_1 + \mathbf{x}_2^T \mathbf{L}_1 \mathbf{x}_2} + \gamma \|\mathbf{x} - (\mathbf{x}_1 + \mathbf{x}_2)\|_2^2, \quad (13)$$

where γ is a regularization parameter that determines the importance of the regularization term in the objective function. In the same way, problems (8) and (9) can also be written in the presence of noise. For example, (9) can be changed as

$$\underset{\mathbf{x}_1, \mathbf{x}_2}{\text{minimize}} \quad \frac{\mathbf{x}_1^T \tilde{\mathbf{L}}_1 \mathbf{x}_1 + \mathbf{x}_2^T \tilde{\mathbf{L}}_2 \mathbf{x}_2}{\mathbf{x}_1^T \tilde{\mathbf{L}}_2 \mathbf{x}_1 + \mathbf{x}_2^T \tilde{\mathbf{L}}_1 \mathbf{x}_2} + \gamma \|\mathbf{z} - (\mathbf{x}_1 + \mathbf{x}_2)\|_2^2 \quad (14)$$

s.t. $\bar{x}_1 = \bar{x}_2 = 0.$

Moreover, problem (7) can be generalized to the case of K graphs. Suppose that $\mathcal{G}_i, i = 1, \dots, K$ are undirected graphs with Laplacian matrices \mathbf{L}_i , and consider \mathbf{x}_i as a smooth graph signal on \mathcal{G}_i . Therefore, the optimization problem to separate the signals is

$$\underset{\mathbf{x}_1, \dots, \mathbf{x}_K}{\text{minimize}} \quad \frac{\sum_{1 \leq i \leq K} \mathbf{x}_i^T \mathbf{L}_i \mathbf{x}_i}{\sum_{1 \leq i \neq j \leq K} \mathbf{x}_i^T \mathbf{L}_j \mathbf{x}_i} \quad \text{s.t.} \quad \mathbf{x} = \sum_{i=1}^K \mathbf{x}_i. \quad (15)$$

However, for $K > 2$, there is no proof for the uniqueness of the solution.

Similarly, problems (8), (9), (13) and (14) can be generalized to the case of K graphs.

IV. A CLOSED-FORM FORMULA FOR THE ESTIMATION ERROR IN CASE OF COMPLEMENT GRAPHS

A type of two graphs that are appropriately different from each other is complement graphs [20]. Since the original signals \mathbf{x}_1 and \mathbf{x}_2 are assumed to be smooth on their own graphs, it is expected that the more the two graphs spectrally differ, the more likely that the signals are non-smooth on the graphs of the other one, and hence a better improvement in separation in both methods. This section is devoted to complement graphs, which represent an extreme case where two graphs differ completely in the spectral domain. In this section, the graph \mathcal{G}_1 is assumed to be an undirected binary graph and \mathcal{G}_2 is assumed to be its complement. In this case, a closed-form formula for the estimation errors of both (6) and (9) can be obtained in terms of the frequency components of the source signals, which can provide an explanation for why the separation methods work well for smooth and bandlimited source signals.

The complement of an undirected binary graph $\mathcal{G} = (\mathcal{V}, \mathcal{E}, \mathbf{W})$ is the graph $\bar{\mathcal{G}} = (\mathcal{V}, \bar{\mathcal{E}}, \bar{\mathbf{W}})$, which has the same set of nodes but its edge set $\bar{\mathcal{E}}$ is the complement of \mathcal{E} with respect to the set of all unordered pairs $\mathcal{V} \times \mathcal{V}$ and therefore, $\mathbf{W} + \bar{\mathbf{W}} = \mathbf{1}\mathbf{1}^T - \mathbf{I}$. In other words, there is an edge between two nodes in $\bar{\mathcal{G}}$ if and only if there is not an edge between those nodes in \mathcal{G} [20].

If two graphs are complement, they will be structurally very different. This is shown by the following lemma.

Lemma 1 ([20, Chapter 1]). *Let \mathcal{G}_1 and \mathcal{G}_2 be two binary complement graphs with N nodes. If \mathbf{v}_i is a Laplacian*

eigenvector of \mathcal{G}_1 with the corresponding eigenvalue λ_i and if \mathbf{v}_i is orthogonal to $\mathbf{1}$, then \mathbf{v}_i will also be a Laplacian eigenvector of \mathcal{G}_2 with the corresponding eigenvalue $N - \lambda_i$.

Therefore, the GFT basis of \mathcal{G}_1 corresponding to lower frequencies is the GFT basis of \mathcal{G}_2 corresponding to higher frequencies and vice versa. This would help the separation processes that are based on the smoothness of signals on their own graphs.

Now, let \mathcal{G}_1 and \mathcal{G}_2 be two connected graphs that are complement and let $0 = \lambda_1 < \lambda_2 \leq \dots \leq \lambda_N$ be the eigenvalues of \mathbf{L}_1 corresponding to the orthonormal eigenvectors $\frac{1}{\sqrt{N}}\mathbf{1}, \mathbf{v}_2, \dots, \mathbf{v}_N$. Based on Lemma 1 and definitions $\mathbf{V}_1 \triangleq [\frac{1}{\sqrt{N}}\mathbf{1}, \mathbf{v}_2, \dots, \mathbf{v}_N]$ and $\mathbf{V}_2 \triangleq [\frac{1}{\sqrt{N}}\mathbf{1}, \mathbf{v}_N, \dots, \mathbf{v}_2]$, the eigenvalue decomposition of \mathbf{L}_1 and \mathbf{L}_2 can be written as $\mathbf{L}_1 = \mathbf{V}_1 \text{diag}(0, \lambda_2, \dots, \lambda_N) \mathbf{V}_1^T$ and $\mathbf{L}_2 = \mathbf{V}_2 \text{diag}(0, N - \lambda_N, \dots, N - \lambda_2) \mathbf{V}_2^T$. The following two theorems express the estimation errors of (4) and (8), respectively.

Theorem 2. Let \mathbf{x}_1^* and \mathbf{x}_2^* be two source signals on complement graphs \mathcal{G}_1 and \mathcal{G}_2 whose GFT coefficients are $\mathbf{V}_1^T \mathbf{x}_1^* = [0, \hat{x}_{12}^*, \dots, \hat{x}_{1N}^*]^T$ and $\mathbf{V}_2^T \mathbf{x}_2^* = [0, \hat{x}_{22}^*, \dots, \hat{x}_{2N}^*]^T$, respectively. Moreover, let $\mathbf{x} \triangleq \mathbf{x}_1^* + \mathbf{x}_2^*$. If $(\mathbf{x}_1, \mathbf{x}_2)$ is the solution of (4) with $\mathbf{z} = \mathbf{x}$, then

$$\|\mathbf{x}_1^* - \mathbf{x}_1\|_2^2 = \|\mathbf{x}_2^* - \mathbf{x}_2\|_2^2 = \sum_{i=2}^N \left(\frac{\lambda_i \hat{x}_{1i}^* - (N - \lambda_i) \hat{x}_{2,N-i+2}^*}{N} \right)^2 \quad (16)$$

The proof is left to Appendix B.

There is a similar result for (9), which is provided in the following theorem.

Theorem 3. Let \mathbf{x}_1^* and \mathbf{x}_2^* be as in Theorem 2. Let $(\mathbf{x}_1, \mathbf{x}_2)$ be the solution of problem (8), and J^* be its optimum value. If $\mathbf{L}_1 \mathbf{x} \neq \mathbf{L}_2 \mathbf{x}$, then

$$\|\mathbf{x}_1^* - \mathbf{x}_1\|_2^2 = \|\mathbf{x}_2^* - \mathbf{x}_2\|_2^2 = \left(\frac{1 + J^*}{1 - J^*} \right)^2 \sum_{i=2}^N \left(\frac{(\lambda_i - \frac{J^* N}{1 + J^*}) \hat{x}_{1i}^* - (\frac{N}{1 + J^*} - \lambda_i) \hat{x}_{2,N-i+2}^*}{N} \right)^2 \quad (17)$$

The proof is left to Appendix C.

Remark: The proof techniques of Theorems 2 and 3 can be applied to obtain the estimation error in case of two weighted graphs with Laplacian matrices \mathbf{L}_1 and \mathbf{L}_2 , in which $\mathbf{L}_1 + \mathbf{L}_2 = N\mathbf{I} - \mathbf{1}\mathbf{1}^T$, or any other cases in which both graphs have the same set of Laplacian eigenvectors.

Similar equations can be derived for the estimation errors of (6) and (9), which are presented in the following theorems. Since their proofs are similar to Theorems 2 and 3, they are left to the reader.

Theorem 4. Let \mathbf{x}_1^* and \mathbf{x}_2^* be as in Theorem 2. If $(\mathbf{x}_1, \mathbf{x}_2)$ is the solution of problem (6), then

$$\|\mathbf{x}_1^* - \mathbf{x}_1\|_2^2 = \|\mathbf{x}_2^* - \mathbf{x}_2\|_2^2 = \sum_{i=2}^N \left(\frac{w_i \hat{x}_{1i}^* - w_{N-i+2} \hat{x}_{2,N-i+2}^*}{w_i + w_{N-i+2}} \right)^2 \quad (18)$$

The above formula shows that the low-frequency components of the source signals \mathbf{x}_1^* and \mathbf{x}_2^* appear with low coefficients in the estimation error of problem (6). Therefore, for smooth signals, for which only low-frequency components have significant values, the error of problem (6) would be small.

Theorem 5. Let \mathbf{x}_1^* and \mathbf{x}_2^* be as in Theorem 3. If $(\mathbf{x}_1, \mathbf{x}_2)$ is the solution of problem (9), then

$$\|\mathbf{x}_1^* - \mathbf{x}_1\|_2^2 = \|\mathbf{x}_2^* - \mathbf{x}_2\|_2^2 = \sum_{i=2}^N \left(\frac{(w_i - J^* w_{N-i+2}) \hat{x}_{1i}^* - (w_{N-i+2} - J^* w_i) \hat{x}_{2,N-i+2}^*}{(w_i + w_{N-i+2})(1 - J^*)} \right)^2 \quad (19)$$

From Theorems 4 and 5, it seems that in the estimation error of (9) compared with (6), the weights corresponding to the frequency components are changed in a way that the error is reduced. This assertion is demonstrated in the simulations of Section V.

V. SIMULATION RESULTS

In this section, our proposed methods are evaluated and compared with the methods of [14], which, to the best of our knowledge, are the only methods that separate smooth graph signals from their summation. Simulations are presented in six different experiments to investigate different scenarios. Graph Signal Processing Toolbox (GSPBox) [21] is used to generate different random graphs in each experiment.

A. Experiment 1: The separation performances of (8) and (9)

In this experiment, the performances of our proposed methods in (8) and (9) are compared with the methods of [14] presented in (4) and (6). To generate a smooth signal \mathbf{x}_i on graph \mathcal{G}_i , the second and third eigenvectors of \mathbf{L}_i are linearly combined with random coefficients chosen i.i.d. from uniform distribution between 0 and 1. Then $\mathbf{x} = \mathbf{x}_1 + \mathbf{x}_2$ is given to the aforementioned methods to reconstruct the original smooth signals \mathbf{x}_1 and \mathbf{x}_2 .

To evaluate the separation performance, signal-to-noise ratio (SNR) is used, which for the i -th estimated signal, $\mathbf{x}_i^{\text{est}}$, is defined as $\text{SNR}_i \triangleq 20 \log_{10}(\|\mathbf{x}_i\|_2 / \|\mathbf{x}_i - \mathbf{x}_i^{\text{est}}\|_2)$. Then SNR_i 's are averaged over all sources, $\text{SNR}_{\text{avg}} \triangleq \frac{1}{K} \sum_{i=1}^K \text{SNR}_i$. Finally, after repeating each simulation several times, SNR_{avg} 's are averaged over the simulations, and their average is denoted by $\overline{\text{SNR}}_{\text{avg}}$, which is reported as the performance index.

At first, the performances of (8) and (4) are compared over two random graphs with the same type, which are connected Erdos-Renyi graphs [22] with N nodes and edge probability $p = 15/N$. Figure 1 shows $\overline{\text{SNR}}_{\text{avg}}$ of (8) and (4) over 200 different simulations versus the number of nodes. The values of $\overline{\text{SNR}}_{\text{avg}}$ in this figure indicate the superiority of our proposed method in (8) compared with (4).

In another simulation, the performances of (6) and (9) are evaluated over two different types of random graphs: a connected Erdos-Renyi graph with N nodes and edge probability $p = 25/N$ and a connected sensor graph [23] with N nodes. As in [14], the weights in these methods, w_i 's, are chosen as

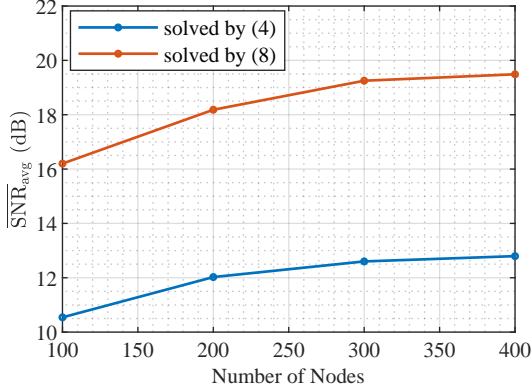


Fig. 1: $\overline{\text{SNR}}_{\text{avg}}$ of the methods (4) and (8) over 2 Erdos-Renyi graphs with respect to the number of nodes.

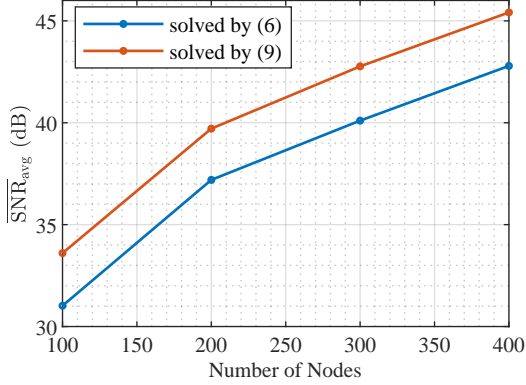


Fig. 2: $\overline{\text{SNR}}_{\text{avg}}$ of the methods (6) and (9) over 2 different graph types with respect to the number of nodes.

$w_i = (i-2)*40+1$ for $i = 2, \dots, N$. Figure 2 shows $\overline{\text{SNR}}_{\text{avg}}$ of methods (6) and (9) over 200 different simulations versus the number of nodes. As seen in this figure, our proposed method in (9) performs better than (6).

B. Experiment 2: The separation performance of (9) with respect to the number of non-zero frequency components

In this experiment, the performance of our proposed method in (9) is evaluated with respect to the number of non-zero frequency components of the source signals and is compared with (6). For this purpose, signals are generated similar to Experiment 1 but with a different number of non-zero frequency components. More precisely, \mathbf{x}_i with s non-zero frequency components is set to be equal to the linear combination of the first s eigenvectors of \mathbf{L}_i (except the first eigenvector) with random coefficients chosen i.i.d. from uniform distribution between 0 and 1. The graphs are a connected sensor graph and a connected Erdos-Renyi graph with $N = 250$ nodes and edge probability $p = 0.1$. The weights in (9) and (6) are chosen similar to Experiment 1. Figure 3 shows $\overline{\text{SNR}}_{\text{avg}}$, averaged over 40 different simulations, with respect to the number of non-zero frequency components. As can be seen in this figure, when the number of non-zero frequency components increases,

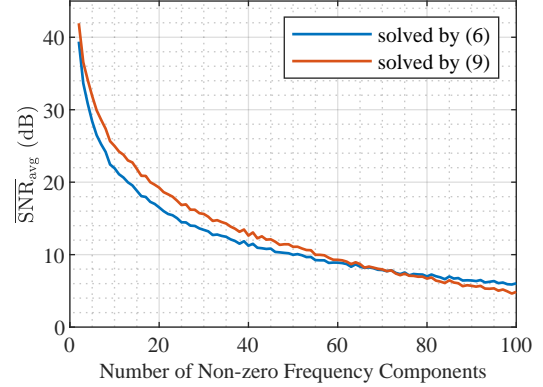


Fig. 3: $\overline{\text{SNR}}_{\text{avg}}$ of methods (6) and (9) with respect to the number of non-zero frequency components.

$\overline{\text{SNR}}_{\text{avg}}$ decreases due to the decrease in the smoothness of the source signals. However, our proposed method still performs better than (6). But when the number of frequency components exceeds a limit (where the signals are not nearly smooth), the performance of our proposed method becomes weaker than (6).

C. Experiment 3: The separation performance of (14) in the presence of noise

In this experiment, the performance of our proposed method is evaluated in the presence of noise. As mentioned earlier, in this case the optimization problem (14) can be used. Moreover, our proposed method is compared with the method of [14], which for two graphs in the presence of noise is

$$\begin{aligned} & \underset{\mathbf{x}_1, \mathbf{x}_2}{\text{minimize}} \quad \|\mathbf{z} - (\mathbf{x}_1 + \mathbf{x}_2)\|_2^2 + \gamma_1 \mathbf{x}_1^T \mathbf{L}_1 \mathbf{x}_1 + \gamma_2 \mathbf{x}_2^T \mathbf{L}_2 \mathbf{x}_2 \\ & \text{s.t.} \quad \bar{x}_1 = \bar{x}_2 = 0, \end{aligned} \quad (20)$$

where γ_1 and γ_2 are regularization parameters. Similar to (14), \mathbf{L}_1 and \mathbf{L}_2 can be replaced by $\tilde{\mathbf{L}}_1$ and $\tilde{\mathbf{L}}_2$, which are used in this experiment. For simulation, the graphs are a connected sensor graph and a connected Erdos-Renyi graph with $N = 250$ nodes and edge probability $p = 0.1$. After generating smooth source signals \mathbf{x}_1 and \mathbf{x}_2 similar to Experiment 1, the summation signal $\mathbf{x}_1 + \mathbf{x}_2$ is corrupted by adding a white Gaussian noise $\mathbf{n} \sim \mathcal{N}(\mathbf{0}, \sigma^2 \mathbf{I})$. Finally, methods (14) and (20) are used to recover source signals from the noisy summation signal $\mathbf{x} \triangleq \mathbf{x}_1 + \mathbf{x}_2 + \mathbf{n}$. In (14) and (20), the regularization parameters γ and $\gamma_1 = \gamma_2$ are set equal to 0.0001 and 0.0025, respectively. These values are empirically chosen based on minimizing the error in the simulations. The weights in all methods are chosen similar to Experiment 1. To solve the optimization problem (14), the gradient descent method with step size $\mu = \frac{1}{t}$ is used, where t is the iteration number.

Figure 4 shows $\overline{\text{SNR}}_{\text{avg}}$, averaged over 100 different simulations, versus $\overline{\text{SNR}}_{\text{input}}$, which is defined as $\text{SNR}_{\text{input}} = 20 \log_{10}(\|\mathbf{x} - \mathbf{n}\|_2 / \|\mathbf{n}\|_2)$ and averaged over simulations. As seen in Fig. 4, both (14) and (20) are robust against noise, i.e. do not change significantly with respect to the noise variance, and in lower input SNR's they perform better than

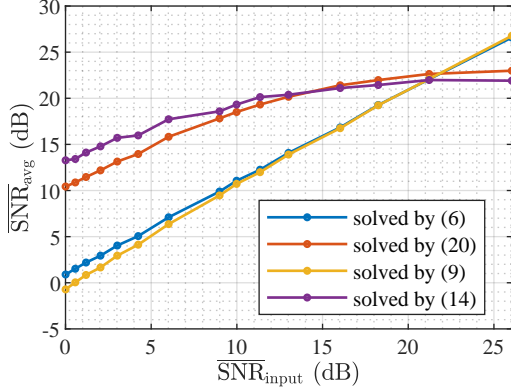


Fig. 4: $\overline{\text{SNR}}_{\text{avg}}$ of methods (6), (9), (14) and (20) with respect to $\overline{\text{SNR}}_{\text{input}}$.

(6) and (9). Moreover, our proposed method in (14) has a better performance compared with the other methods in lower input SNR's.

D. Experiment 4: The separation performance in the case of compliment graphs

In this experiment, the performances of (6) and (9) are evaluated in case of complement graphs, whose theoretical results were provided in the previous section. For this purpose, at first, a connected Erdos-Renyi graph is generated with N nodes and edge probability $p = 0.5$ and then, its complement graph is constructed. These two graphs are considered as the main graphs in (6) and (9). Generation of \mathbf{x}_i 's and all parameters are similar to Experiments 1 and 2. Figures 5a and 5b show the performances of these methods with respect to the number of nodes and the number of non-zero frequency components, respectively. Both figures indicate that our proposed method in (9) performs better than (6). Furthermore, compared with Figs. 1 and 2, both methods perform better in case of complement graphs. This is because, as explained in the previous section, complementary graphs have different spectral properties, ensuring that a smooth signal on one is non-smooth on the other, and this helps the separation process.

E. Experiment 5: The separation performance of (15) in case of more than two source signals

In this experiment, for the case of more than two source signals, the performance of our proposed method, *i.e.* (15), is evaluated and compared with the method of [14], which for more than two source signals is

$$\underset{\mathbf{x}_1, \dots, \mathbf{x}_K}{\text{minimize}} \quad \sum_{1 \leq i \leq K} \mathbf{x}_i^T \mathbf{L}_i \mathbf{x}_i \quad \text{s.t.} \quad \mathbf{x} = \sum_{i=1}^K \mathbf{x}_i. \quad (21)$$

For simulation, four different types of random graphs with N nodes are generated: an Erdos-Renyi graph with edge probability $p = 25/N$, a sensor graph, a random regular graph [24] with degree parameter 20, and a stochastic block

TABLE I: Image separation quality based on SNR (dB).

	solved by (4)		solved by (8)	
	SNR ₁	SNR ₂	SNR ₁	SNR ₂
set 1	16.0186	16.0682	16.0244	16.0739
set 2	10.0104	14.8041	10.0233	14.8170

model graph [25] with 2 clusters. After generating source signals $\mathbf{x}_1, \dots, \mathbf{x}_4$ similar to Experiments 1 and 2, the summation signal $\mathbf{x} \triangleq \mathbf{x}_1 + \dots + \mathbf{x}_4$ is given to (15) and (21) to reconstruct the source signals. In both methods, $\tilde{\mathbf{L}}_i$'s are used instead of \mathbf{L}_i 's with $w_i = (i - 2) * 40 + 1$ for $i = 2, \dots, N$ (in the simulation related to Fig. 6b, N is equal to 100). To solve the optimization problem (15), the gradient descent method with step size $\mu = 1.5$ is used and after updating the signals $\mathbf{x}_1, \dots, \mathbf{x}_4$ in each iteration, they are projected onto the space $\{(\mathbf{x}_1, \dots, \mathbf{x}_4) \in \mathbb{R}^N : \mathbf{x}_1 + \dots + \mathbf{x}_4 = \mathbf{x}\}$. Figures 6a and 6b show $\overline{\text{SNR}}_{\text{avg}}$, averaged over 20 different simulations, with respect to the number of nodes and the number of non-zero frequency components, respectively. As seen in Fig. 6a, the results show again the superiority of our proposed methods. Moreover, Fig. 6b indicates that in lower number of non-zero frequency components, our proposed methods performs better, but by increasing the number of non-zero frequency components its performance drops faster.

F. Experiment 6: A proof of concept with real data

In this experiment, similar to Experiment 6 of [14], the performance of our proposed method is evaluated in separation of images. Since the graphs of images are often not available in real-world applications, this experiment serves only as a visual proof of concept. The procedure of this simulation is explained in [14]. Briefly, at first a 64 by 64 pixel image is converted to a vector with 4096 entries, which are between 0 and 255, as a graph signal \mathbf{x}_i and then, a graph is assigned to the signal so that the signal is approximately smooth on that graph. To create such a graph for the signal \mathbf{x}_i , each pixel is connected to its eight neighbours and the edge weight between the node k and j is set equal to $w_{kj} = 1/(|(\mathbf{x}_i)_k - (\mathbf{x}_i)_j| + 0.001)$, where $(\mathbf{x}_i)_k$ and $(\mathbf{x}_i)_j$ are the k -th and j -th entries of \mathbf{x}_i , respectively. Finally, $\mathbf{x} \triangleq \mathbf{x}_1 + \mathbf{x}_2$ and the graphs associated to \mathbf{x}_1 and \mathbf{x}_2 are given to (8) and the estimated signals $\tilde{\mathbf{x}}_1$ and $\tilde{\mathbf{x}}_2$ are obtained. To show the estimated images, after adding 127 as a constant to each estimated signal (because $\tilde{\mathbf{x}}_1$ and $\tilde{\mathbf{x}}_2$ are zero mean), the values lower than 0 and greater than 255 are set equal to 0 and 255, respectively. Figure 7 shows the original and estimated images for two different image sets. As seen in this figure, the estimated images are almost identical to the original images. Moreover, the SNR of each estimated signal is shown in Table I, which for $\tilde{\mathbf{x}}_i$ is defined as $\text{SNR}_i = 20 \log_{10}(\|\mathbf{z}_i\|_2 / \|\mathbf{z}_i - \tilde{\mathbf{x}}_i\|_2)$, where $\mathbf{z}_i \triangleq \mathbf{x}_i - \bar{x}_i \mathbf{1}$. The SNR values in this table indicate that the separation of the images is done to an acceptable extent. But the SNR values are lower than the previous experiments. This is because that, as stated in [14], the frequency components of the graph signals in this experiment are non-zero in a wide range, contrary to the previous experiments in which only some of the first frequency components were non-zero.

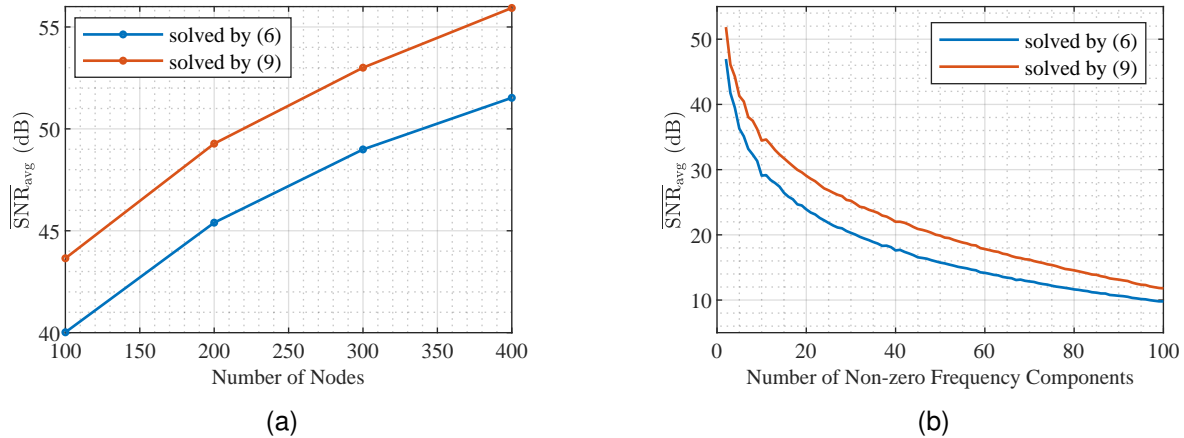


Fig. 5: $\overline{\text{SNR}}_{\text{avg}}$ of methods (6) and (9) in case of complement graphs (a) with respect to the number of nodes. (b) with respect to the number of non-zero frequency components.

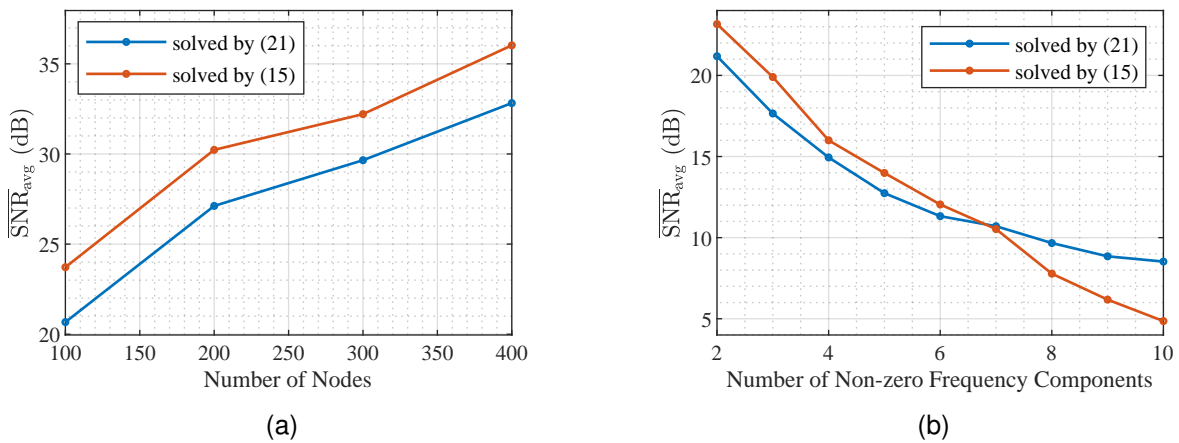


Fig. 6: $\overline{\text{SNR}}_{\text{avg}}$ of methods (15) and (21) in case of separation four graph signals (a) with respect to the number of nodes. (b) with respect to the number of non-zero frequency components.

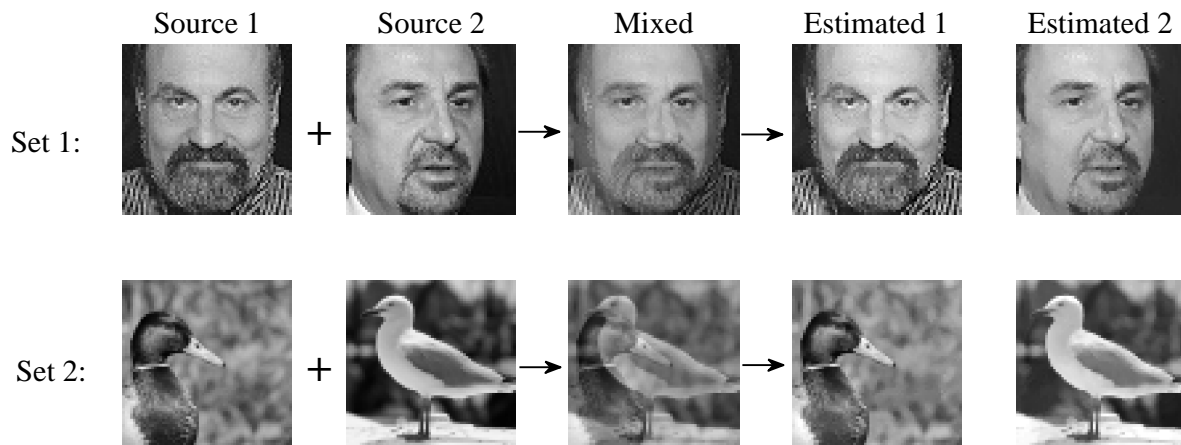


Fig. 7: Separation results by using method (8) for two sets of images.

VI. CONCLUSION

In this paper, an approach was proposed to separate K smooth graph signals from their summation. The objective

function of this optimization approach is based on finding graph signals that are as smooth as possible on their corre-

sponding graph and non-smooth on the other graphs. In the case of $K = 2$, it was shown that the solution of the proposed approach is unique up to the uncertainty of the average values of the signals, and a fixed point algorithm based on KKT conditions was introduced. Moreover, for complement graphs, the exact error formulas were obtained for both our proposed approach and the approach of [14], which, up to our best knowledge, is the only approach in this setting. Simulations demonstrated the efficiency of the proposed methods and its superiority over the other methods in different experiments.

APPENDIX A PROOF OF THEOREM (1)

To prove Theorem 1, we first prove the following lemma.

Lemma 2. *If $\mathbf{L}_1\mathbf{x} \neq \mathbf{L}_2\mathbf{x}$, the optimum value of problem (7) is strictly smaller than one.*

Proof. Let $J(\mathbf{x}_1, \mathbf{x}_2)$ and J^* be the objective function and the minimum value of problem (7). It is easy to see that $J(\mathbf{x}_2, \mathbf{x}_1) = (J(\mathbf{x}_1, \mathbf{x}_2))^{-1}$ so $J^* \leq 1$. If $J^* = 1$, then

$$J(\mathbf{x}_1, \mathbf{x} - \mathbf{x}_1) = 1 \quad \forall \mathbf{x}_1 \in \mathbb{R}^N. \quad (22)$$

Otherwise, if there exists \mathbf{x}_1 such that $J(\mathbf{x}_1, \mathbf{x} - \mathbf{x}_1) > 1$, then $J(\mathbf{x} - \mathbf{x}_1, \mathbf{x}_1) < 1$, and this implies $J^* < 1$, which is a contradiction. Therefore, $\nabla_{\mathbf{x}_1} J(\mathbf{x}_1, \mathbf{x} - \mathbf{x}_1) = \mathbf{0}$ and

$$(\mathbf{L}_1 + \mathbf{L}_2)\mathbf{x}_1 - \mathbf{L}_2\mathbf{x} - J(\mathbf{x}_1, \mathbf{x} - \mathbf{x}_1)((\mathbf{L}_1 + \mathbf{L}_2)\mathbf{x}_1 - \mathbf{L}_1\mathbf{x}) = \mathbf{0}. \quad (23)$$

Since $J(\mathbf{x}_1, \mathbf{x} - \mathbf{x}_1) = 1$, then $\mathbf{L}_1\mathbf{x} = \mathbf{L}_2\mathbf{x}$, which is a contradiction with the lemma's assumption. So, $J^* < 1$. \square

Proof of Theorem 1: The Lagrangian function of problem (7) is

$$L(\mathbf{x}_1, \mathbf{x}_2, \boldsymbol{\mu}) = J(\mathbf{x}_1, \mathbf{x}_2) + \boldsymbol{\mu}^T(\mathbf{x}_1 + \mathbf{x}_2 - \mathbf{x}), \quad (24)$$

where $\boldsymbol{\mu} \in \mathbb{R}^N$ is the vector of Lagrange multipliers. Therefore, $\nabla_{\mathbf{x}_1} L$ equals

$$2 \frac{\mathbf{L}_1\mathbf{x}_1(\mathbf{x}_1^T \mathbf{L}_2\mathbf{x}_1 + \mathbf{x}_2^T \mathbf{L}_1\mathbf{x}_2) - \mathbf{L}_2\mathbf{x}_1(\mathbf{x}_1^T \mathbf{L}_1\mathbf{x}_1 + \mathbf{x}_2^T \mathbf{L}_2\mathbf{x}_2)}{(\mathbf{x}_1^T \mathbf{L}_2\mathbf{x}_1 + \mathbf{x}_2^T \mathbf{L}_1\mathbf{x}_2)^2} + \boldsymbol{\mu} \quad (25)$$

$$= 2 \frac{\mathbf{L}_1\mathbf{x}_1 - J(\mathbf{x}_1, \mathbf{x}_2)\mathbf{L}_2\mathbf{x}_1}{\mathbf{x}_1^T \mathbf{L}_2\mathbf{x}_1 + \mathbf{x}_2^T \mathbf{L}_1\mathbf{x}_2} + \boldsymbol{\mu}, \quad (26)$$

and a similar equation holds for $\nabla_{\mathbf{x}_2} L$. Suppose both $(\mathbf{x}_1, \mathbf{x}_2)$ and $(\tilde{\mathbf{x}}_1, \tilde{\mathbf{x}}_2)$ are the solutions of problem (7). Hence, the KKT conditions [19] imply that

$$\begin{cases} 2 \frac{\mathbf{L}_1\mathbf{x}_1 - J(\mathbf{x}_1, \mathbf{x}_2)\mathbf{L}_2\mathbf{x}_1}{\mathbf{x}_1^T \mathbf{L}_2\mathbf{x}_1 + \mathbf{x}_2^T \mathbf{L}_1\mathbf{x}_2} + \boldsymbol{\mu} = \mathbf{0} \\ 2 \frac{\mathbf{L}_2\mathbf{x}_2 - J(\mathbf{x}_1, \mathbf{x}_2)\mathbf{L}_1\mathbf{x}_2}{\mathbf{x}_1^T \mathbf{L}_2\mathbf{x}_1 + \mathbf{x}_2^T \mathbf{L}_1\mathbf{x}_2} + \boldsymbol{\mu} = \mathbf{0} \\ \mathbf{x}_1 + \mathbf{x}_2 = \mathbf{x} \end{cases}, \quad (27)$$

$$\begin{cases} 2 \frac{\mathbf{L}_1\tilde{\mathbf{x}}_1 - J(\tilde{\mathbf{x}}_1, \tilde{\mathbf{x}}_2)\mathbf{L}_2\tilde{\mathbf{x}}_1}{\tilde{\mathbf{x}}_1^T \mathbf{L}_2\tilde{\mathbf{x}}_1 + \tilde{\mathbf{x}}_2^T \mathbf{L}_1\tilde{\mathbf{x}}_2} + \tilde{\boldsymbol{\mu}} = \mathbf{0} \\ 2 \frac{\mathbf{L}_2\tilde{\mathbf{x}}_2 - J(\tilde{\mathbf{x}}_1, \tilde{\mathbf{x}}_2)\mathbf{L}_1\tilde{\mathbf{x}}_2}{\tilde{\mathbf{x}}_1^T \mathbf{L}_2\tilde{\mathbf{x}}_1 + \tilde{\mathbf{x}}_2^T \mathbf{L}_1\tilde{\mathbf{x}}_2} + \tilde{\boldsymbol{\mu}} = \mathbf{0} \\ \tilde{\mathbf{x}}_1 + \tilde{\mathbf{x}}_2 = \mathbf{x} \end{cases}, \quad (28)$$

where $\boldsymbol{\mu}, \tilde{\boldsymbol{\mu}} \in \mathbb{R}^N$ are the vectors of Lagrange multipliers. Combining the first two equations of (27) and (28), and considering $J(\mathbf{x}_1, \mathbf{x}_2) = J(\tilde{\mathbf{x}}_1, \tilde{\mathbf{x}}_2) = J^*$, leads to

$$\begin{cases} \mathbf{L}_1\mathbf{x}_1 - J^*\mathbf{L}_2\mathbf{x}_1 = \mathbf{L}_2\mathbf{x}_2 - J^*\mathbf{L}_1\mathbf{x}_2 \\ \mathbf{L}_1\tilde{\mathbf{x}}_1 - J^*\mathbf{L}_2\tilde{\mathbf{x}}_1 = \mathbf{L}_2\tilde{\mathbf{x}}_2 - J^*\mathbf{L}_1\tilde{\mathbf{x}}_2 \end{cases}. \quad (29)$$

By subtracting the first equation from the second one,

$$\mathbf{L}_1\mathbf{e}_1 - J^*\mathbf{L}_2\mathbf{e}_1 = \mathbf{L}_2\mathbf{e}_2 - J^*\mathbf{L}_1\mathbf{e}_2, \quad (30)$$

where $\mathbf{e}_i \triangleq \mathbf{x}_i - \tilde{\mathbf{x}}_i$, $i = 1, 2$. From the third equations in (27) and (28), $\mathbf{e}_1 + \mathbf{e}_2 = \mathbf{0}$. Therefore,

$$(\mathbf{L}_1 + \mathbf{L}_2)(1 - J^*)\mathbf{e}_1 = \mathbf{0}. \quad (31)$$

According to Lemma 2, $J^* < 1$, so, $(\mathbf{L}_1 + \mathbf{L}_2)\mathbf{e}_1 = \mathbf{0}$. Because both graphs are connected, both \mathbf{L}_1 and \mathbf{L}_2 have only one zero eigenvalue with corresponding eigenvector $\mathbf{1}$. Therefore, the only possible values for \mathbf{e}_1 is the form $\mathbf{e}_1 = c\mathbf{1}$, where c is a scalar. And hence, $\mathbf{e}_2 = -c\mathbf{1}$. This means that the possible solutions of problem (7) only differ in their DC values. \square

APPENDIX B PROOF OF THEOREM (2)

According to [14, Eq. (16)], $\mathbf{L}_1\mathbf{x}_1 = \mathbf{L}_2\mathbf{x}_2$, which in the GFT domain can be written as

$$\sum_{i=2}^N \lambda_i \hat{x}_{1i} \mathbf{v}_i = \sum_{i=2}^N (N - \lambda_i) \hat{x}_{2, N-i+2} \mathbf{v}_i, \quad (32)$$

where $\mathbf{V}_1^T \mathbf{x}_1 = [0, \hat{x}_{12}, \dots, \hat{x}_{1N}]^T$ and $\mathbf{V}_2^T \mathbf{x}_2 = [0, \hat{x}_{22}, \dots, \hat{x}_{2N}]^T$. Since $\mathbf{v}_2, \dots, \mathbf{v}_N$ are orthonormal, (32) is simplified to

$$\lambda_i \hat{x}_{1i} = (N - \lambda_i) \hat{x}_{2, N-i+2} \quad i = 2, \dots, N. \quad (33)$$

On the other hand, $\mathbf{x}_1 + \mathbf{x}_2 = \mathbf{x}_1^* + \mathbf{x}_2^*$ and therefore, $\hat{x}_{1i} + \hat{x}_{2, N-i+2} = \hat{x}_{1i}^* + \hat{x}_{2, N-i+2}^*$, which together with (33) leads to

$$\hat{x}_{1i} = \frac{N - \lambda_i}{N} (\hat{x}_{1i}^* + \hat{x}_{2, N-i+2}^*) \quad i = 2, \dots, N, \quad (34)$$

$$\hat{x}_{2, N-i+2} = \frac{\lambda_i}{N} (\hat{x}_{1i}^* + \hat{x}_{2, N-i+2}^*) \quad i = 2, \dots, N. \quad (35)$$

Moreover, because $\mathbf{v}_2, \dots, \mathbf{v}_N$ are orthonormal,

$$\|\mathbf{x}_j^* - \mathbf{x}_j\|_2^2 = \sum_{i=2}^N (\hat{x}_{ji} - \hat{x}_{ji}^*)^2 \quad j = 1, 2. \quad (36)$$

Finally, by using equations (34) and (35) in (36), Theorem 2 is proved. \square

APPENDIX C PROOF OF THEOREM (3)

Based on (29), $(\mathbf{L}_1 - J^*\mathbf{L}_2)\mathbf{x}_1 = (\mathbf{L}_2 - J^*\mathbf{L}_1)\mathbf{x}_2$. So, similar to Appendix B

$$\sum_{i=2}^N (\lambda_i - J^*(N - \lambda_i)) \hat{x}_{1i} \mathbf{v}_i = \sum_{i=2}^N ((N - \lambda_i) - J^* \lambda_i) \hat{x}_{2, N-i+2} \mathbf{v}_i, \quad (37)$$

where $\mathbf{V}_1^T \mathbf{x}_1 = [0, \hat{x}_{12}, \dots, \hat{x}_{1N}]^T$ and $\mathbf{V}_2^T \mathbf{x}_2 = [0, \hat{x}_{22}, \dots, \hat{x}_{2N}]^T$. This leads to the following equations for $i = 2, \dots, N$:

$$\hat{x}_{1i} = \frac{(N - \lambda_i) - J^* \lambda_i}{N} (\hat{x}_{1i}^* + \hat{x}_{2, N-i+2}^*), \quad (38)$$

$$\hat{x}_{2, N-i+2} = \frac{\lambda_i - J^*(N - \lambda_i)}{N} (\hat{x}_{1i}^* + \hat{x}_{2, N-i+2}^*). \quad (39)$$

Using these equations in (36) proves the theorem. \square

REFERENCES

- [1] D. I. Shuman, S. K. Narang, P. Frossard, A. Ortega, and P. Vandergheynst, "The emerging field of signal processing on graphs: Extending high-dimensional data analysis to networks and other irregular domains," *IEEE Signal Processing Magazine*, vol. 30, no. 3, pp. 83–98, may 2013.
- [2] X. Dong, D. Thanou, P. Frossard, and P. Vandergheynst, "Learning laplacian matrix in smooth graph signal representations," *IEEE Transactions on Signal Processing*, vol. 64, no. 23, pp. 6160–6173, dec 2016.
- [3] P. Comon and C. Jutten, *Handbook of Blind Source Separation: Independent component analysis and applications*. Academic press, 2010.
- [4] J. Miettinen, E. Nitzan, S. A. Vorobyov, and E. Ollila, "Graph signal processing meets blind source separation," *IEEE Transactions on Signal Processing*, vol. 69, pp. 2585–2599, 2021.
- [5] J. Miettinen, S. A. Vorobyov, and E. Ollila, "Blind source separation of graph signals," in *ICASSP 2020 - 2020 IEEE International Conference on Acoustics, Speech and Signal Processing (ICASSP)*. IEEE, may 2020.
- [6] F. Blöchl, A. Kowarsch, and F. J. Theis, "Second-order source separation based on prior knowledge realized in a graph model," in *Latent Variable Analysis and Signal Separation*. Springer Berlin Heidelberg, 2010, pp. 434–441.
- [7] A. Kowarsch, F. Blöchl, S. Bohl, M. Saile, N. Gretz, U. Klingmüller, and F. J. Theis, "Knowledge-based matrix factorization temporally resolves the cellular responses to IL-6 stimulation," *BMC Bioinformatics*, vol. 11, no. 1, nov 2010.
- [8] A. Einizade, S. H. Sardouie, and M. Shamsollahi, "Simultaneous graph learning and blind separation of graph signal sources," *IEEE Signal Processing Letters*, vol. 28, pp. 1495–1499, 2021.
- [9] A. Einizade and S. H. Sardouie, "A unified approach for simultaneous graph learning and blind separation of graph signal sources," *IEEE Transactions on Signal and Information Processing over Networks*, vol. 8, pp. 543–555, 2022.
- [10] —, "Robust blind separation of smooth graph signals using minimization of graph regularized mutual information," *Digital Signal Processing*, vol. 132, p. 103792, dec 2022.
- [11] —, "Joint graph learning and blind separation of smooth graph signals using minimization of mutual information and laplacian quadratic forms," *IEEE Transactions on Signal and Information Processing over Networks*, vol. 9, pp. 35–47, 2023.
- [12] F. J. Iglesias, S. Segarra, S. Rey-Escudero, A. G. Marques, and D. Ramirez, "Demixing and blind deconvolution of graph-diffused sparse signals," in *2018 IEEE International Conference on Acoustics, Speech and Signal Processing (ICASSP)*. IEEE, apr 2018.
- [13] F. J. I. Garcia, S. Segarra, and A. G. Marques, "Blind demixing of diffused graph signals," *arXiv*, 2020. [Online]. Available: <https://arxiv.org/abs/2012.13301>
- [14] S. Mohammadi, M. Babaie-Zadeh, and D. Thanou, "Graph signal separation based on smoothness or sparsity in the frequency domain," *IEEE Transactions on Signal and Information Processing over Networks*, pp. 1–10, 2023.
- [15] P. Humbert, B. Le Bars, L. Oudre, A. Kalogeratos, and N. Vayatis, "Learning laplacian matrix from graph signals with sparse spectral representation," *The Journal of Machine Learning Research*, vol. 22, no. 1, pp. 8766–8812, 2021.
- [16] U. Von Luxburg, "A tutorial on spectral clustering," *Statistics and computing*, vol. 17, pp. 395–416, 2007.
- [17] M.-H. A. Yarandi and M. Babaie-Zadeh, "A closed-form solution for graph signal separation based on smoothness," *IEEE Transactions on Signal and Information Processing over Networks*, vol. 9, pp. 823–824, 2023.
- [18] P. Xanthopoulos, P. M. Pardalos, and T. B. Trafalis, "Linear discriminant analysis," in *SpringerBriefs in Optimization*. Springer New York, nov 2012, pp. 27–33.
- [19] J. Nocedal and S. J. Wright, *Numerical Optimization*. Springer New York, 2006.
- [20] A. E. Brouwer and W. H. Haemers, *Spectra of graphs*. Springer Science & Business Media, 2011.
- [21] N. Perraudin, J. Paratte, D. Shuman, L. Martin, V. Kalofolias, P. Vandergheynst, and D. K. Hammond, "Gspbox: A toolbox for signal processing on graphs," 2014.
- [22] P. Erdős, A. Rényi *et al.*, "On the evolution of random graphs," *Publ. Math. Inst. Hung. Acad. Sci.*, vol. 5, no. 1, pp. 17–60, 1960.
- [23] N. P. Mahalik, Ed., *Sensor Networks and Configuration*. Springer Berlin Heidelberg, 2007.
- [24] J. H. Kim and V. H. Vu, "Generating random regular graphs," in *Proceedings of the thirty-fifth annual ACM symposium on Theory of computing*. ACM, jun 2003.
- [25] E. Abbe, "Community detection and stochastic block models: recent developments," *The Journal of Machine Learning Research*, vol. 18, no. 1, pp. 6446–6531, 2017.